Available online at www.sciencedirect.com
ScienceDirect
Journal of Power Sources 160 (2006) 1294–1301
JOURNAL OF POWER SOURCES
www.elsevier.com/locate/jpowsour

Synthesis and electrochemical studies on Al_2O_3 coated $LiNi_{0.5}Co_{0.44}Fe_{0.06}VO_4$ for lithium ion batteries

George Ting-Kuo Fey *, Pandurangan Muralidharan, Yung-Da Cho

Department of Chemical and Materials Engineering, National Central University, Chung-Li, Taiwan 32054, ROC

Received 8 December 2005; received in revised form 6 February 2006; accepted 6 February 2006
Available online 23 March 2006

Abstract

$LiNi_{0.5}Co_{0.44}Fe_{0.06}VO_4$ cathode material has been synthesized by a citric acid:polyethylene glycol polymeric method at 723 K for 5 h in air. The surface of the $LiNi_{0.5}Co_{0.44}Fe_{0.06}VO_4$ was coated with various wt.% of Al_2O_3 by a wet chemical procedure and heat treated 873 K for 2 h in air. The samples were characterized by XRD, FTIR, SEM, and TEM techniques. XRD patterns expose that the complete crystalline phase occurred at 723 K and there was no indication of new peaks for the coated samples. FTIR spectra show that the complete removal of organic residues and the formation of $LiNi_{0.5}Co_{0.44}Fe_{0.06}VO_4$. TG/DTGA results reveal that the formation of $LiNi_{0.5}Co_{0.44}Fe_{0.06}VO_4$ occurred between 480 and 670 K and the complete crystalline occurred at 723 K. SEM micrographs show the various morphological stages of the polymeric intermediates. TEM micrographs of the pristine $LiNi_{0.5}Co_{0.44}Fe_{0.06}VO_4$ reveal that the particle size ranged from 130 to 150 nm and Al_2O_3 coating on the fine particles was compact and had an average thickness of about 15 nm. The charge–discharge experiments were carried out between 2.8 and 4.9 V (versus Li) at a current rate of 0.15 C. The 1.0 wt.% Al_2O_3 coated sample had the best electrochemical performance, with an initial capacity of 65 mAh g^{-1} and capacity retention of 60% after 50 cycles. The electrochemical impedance behavior suggests that the failure of pristine cathode performance is associated with an increase in the impedance growth on the surface of the cathode material upon continuous cycling.

Keywords: Al_2O_3; Coating; Charge–discharge; $LiNi_{0.5}Co_{0.44}Fe_{0.06}VO_4$; Lithium-ion batteries

1. Introduction

In recent years, the need for a lithium ion battery with high voltage and high energy density has become more urgent because of proliferation of advanced portable electronic devices and hybrid vehicles. Transition metal oxides are the most commonly used cathodes in lithium rechargeable batteries because of their characteristic high voltage and high volumetric energy density. Polyanionic vanadate, phosphate and molybdate based materials have attracted a great deal of attention, including inverse spinel $LiMVO_4$ (M = Co, Ni) structured cathode materials, by Fey et al. [1–6], that have superior electrochemical properties, such as high voltage near 5.0 V ($LiNiVO_4$) and 4.5 V ($LiCoVO_4$), compared to the commercially available cathode materials. The structure consists of Li^+ ions residing in octahedral sites and Co^{2+}, Ni^{2+} ions and V^{5+} ions distributed both in octahedrally and tetrahedrally coordinated sites.

The electrochemical performance of these materials was found to be different in the 5 V region, which is significant since it implies that the presence and sites of nickel atoms in an inverse spinel structure may play an important role in the voltage behavior of these materials. Therefore, several investigations [7–9] on the mixed solid solution of lithium transition metal vanadates of Co^{2+} and Ni^{2+} have been carried out. These $LiCo_yNi_{1-y}VO_4$ compounds also adopted an inverse spinel structure. Schoonman et al. [10–12] demonstrated by doping Cu, Cr and Fe into $LiCoVO_4$ cathode material to improve electronic conductivity as well as electrochemical performance. Hence, we focused our attention to obtaining a mixed composition of $LiNi_{0.5}Co_{0.44}Fe_{0.06}VO_4$ by partial substitution of Ni^{2+} in the octahedral sites by Co^{2+}. Fe^{2+} ions may have an advanced effect on its structural and electrochemical properties.

* Corresponding author. Tel.: +886 3 425 7325; fax: +886 3 425 7325.
E-mail address: gfey@cc.ncu.edu.tw (G.T.-K. Fey).

0378-7753/$ – see front matter © 2006 Elsevier B.V. All rights reserved.
doi:10.1016/j.jpowsour.2006.02.008

The mixed solid solution materials possessed better initial charge capacity, but the capacity retention was deprived. These high-voltage cathode materials are also strong oxidizers that may create electrolyte degradation problems. Recently, many researchers have studied the surface treatment of electrode active materials with inert metal oxide to improve both the cycle stability and rate capability of electrode materials at room and high temperatures. Several works have extensively studied both layered and spinel oxides for improvements in cycling stability by the surface coating technique. Al_2O_3 [13–18], MgO [19], TiO_2 [17,20], ZrO_2 [17,20], and SiO_2 [21] coated to the core material confirmed the enhanced cycling behavior of the cathode. The improved cycling performance and capacity retention of the high fracture-tough coated cathode is assumed to result from the shielding of 3d metal ion diffusion and dissolution into the electrolyte.

In this work, for the first time we have attempted to synthesize $LiNi_{0.5}Co_{0.44}Fe_{0.06}VO_4$ by a citric acid:polyethylene glycol (CA:PEG) polymeric method and coat the core material with various wt.% of Al_2O_3 by a wet chemical process. The polymeric complex derived products were characterized by various techniques and their capacity, cycle stability and impedance growth were construed with respect to cycle number.

2. Experiment

$LiNi_{0.5}Co_{0.44}Fe_{0.06}VO_4$ cathode material was synthesized by a CA:PEG polymeric method. In the synthesis process, the molar ratio of CA:PEG was 3:1. According to the stoichiometric composition, specific amounts of Li_2CO_3, $NiCO_3{\cdot}2Ni(OH)_2{\cdot}4H_2O$, $Co(CH_3COO)_2{\cdot}4H_2O$, $FeCl_2{\cdot}4H_2O$ and NH_4VO_3 (Acros Organics, >98%) combined to produce $LiNi_{0.5}Co_{0.44}Fe_{0.06}VO_4$, were dissolved in the deionized water under constant magnetic stirring at 353 K. Concentrated citric acid solution was slowly added drop wise to the above solution, followed by polyethylene glycol with continuous stirring. The resultant transparent dark brown solution was heated gently at 373 K with continuous stirring for 6 h to remove the excess water. The solution turns a transparent dark green and was allowed to form a polymeric gel. Subsequently, the polymeric gel was heat treated at 423 K in a vacuum oven for 24 h. The dried porous polymeric precursor was heat treated at a ramping rate of 2 K min^{-1} and maintained at 573 K for 3 h in air and 723 K for 5 h in air, with intermediate grinding. Scheme 1, presents the schematic illustration of the complete procedure for the synthesis of $LiNi_{0.5}Co_{0.44}Fe_{0.06}VO_4$ cathode material. The same procedure was followed to prepare undoped $LiNi_{0.5}Co_{0.5}VO_4$ in

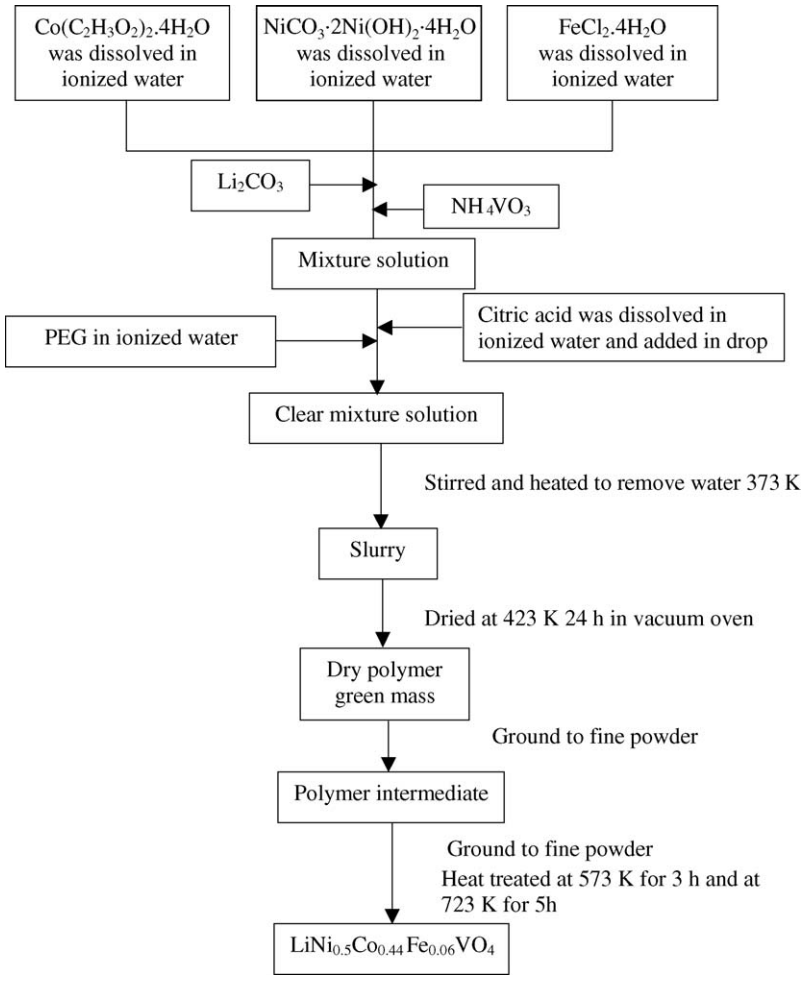

Scheme 1. Schematic for the $LiNi_{0.5}Co_{0.44}Fe_{0.06}VO_4$ prepared by a CA:PEG polymeric route.

order to compare the structural modification with the Fe doped cathode material.

$LiNi_{0.5}Co_{0.44}Fe_{0.06}VO_4$ cathode particles were coated with 1.0, 2.5 and 5.0 wt.% of Al_2O_3 by a wet chemical process. The synthesized cathode particles were dispersed in a beaker containing 0.1 M solution of $NaHCO_3$ solution and ultrasonically agitated for 15 min. The suspension was stirred mechanically for 2 h and the calculated amounts of $Al(NO_3)_3{\cdot}9H_2O$, to form 5.0, 2.5 and 1.0 wt.% of Al_2O_3, were added drop wise slowly under constant stirring. Subsequently, the dispersed solution was stirred for 6 h at room temperature. The dispersed solution was filtered over a Buchner funnel and washed with hot distilled water, in order to remove any excess base and water soluble impurities. The powder was dried for 12 h in a vacuum oven at 423 K and heat treated at 873 K for 2 h in air.

Structural analysis and phase purity were demonstrated by a powder X-ray diffractometer (XRD), Siemens D-5000, Mac Science MXP18, equipped with a nickel-filtered Cu-Kα radiation source (λ = 1.5405 Å). The diffraction patterns were recorded between scattering angles of 15° and 80° in steps of 0.05°. Fourier transform infrared (FTIR) spectra were recorded at room temperature on powdered samples using the KBr wafer technique in a Jasco-410 FTIR instrument. The spectra were recorded with a resolution of 2 cm^{-1} in transmittance mode from 400 to 4000 cm^{-1} and corrected for background. The thermal analysis (TG/DTGA) measurement was carried out on a Perkin-Elmer TGA-7 series thermal analysis system in air at a heating rate of 20 K min^{-1} in the temperature range from 323 to 773 K. The surface morphological studies were carried out on a Hitachi model S-3500V scanning electron microscope (SEM). The microstructures of the particles were examined by a JEOL JEM-200FXII transmission electron microscope (TEM) equipped with a LaB_6 gun. The sample for TEM study was prepared by dispersing the cathode powder in ethanol, placing a drop of the clear solution on a carbon-coated copper grid, and subsequent drying.

The cathodes for electrochemical studies were prepared by a doctor-blade coating method with a slurry of 85 wt.% coated active material, 10 wt.% conductive carbon black and 5 wt.% poly(vinylidene fluoride) as a binder, in *N*-methyl-2-pyrrolidone (*N*MP), as the solvent for the mixture, which was then applied onto an etched aluminum foil current collector and dried at 393 K for 12 h in an oven. The coated cathode foil was then smoothed by pressing it through stainless-steel twin rollers and cut into circular discs 13 mm in diameter.

The electrochemical performance of the above discs were carried out with coin type cells of the 2032 configuration and were assembled in an argon-filled VAC MO40-1 glove box in which the oxygen and water contents were maintained below 2 ppm. Lithium metal (Foote Mineral) was used as the anode and a 1M solution $LiPF_6$ in ethylene carbonate:dimethyl carbonate EC:DMC (1:1 v/v) (Tomiyama Pure Chemical Industries) was used as the electrolyte with a Celgard membrane as the separator. The cells charge–discharge cycles were preformed at a 0.15 C rate between 2.8–4.9 V, at 298 K, in a multi-channel battery tester (Maccor 4000).

Coin cells fully charged to 4.9 V were subjected to impedance measurements at 298 K. The impedance spectra were recorded using a Schlumberger 1286 electrochemical interface and frequency response analyzer (Model 1255), driven by Corrware software (Scribner Associates). The frequency range was 65 KHz–0.001 Hz and the amplitude of the perturbation signal was 20 mV. The impedance spectra were analyzed with Z-view software (Scribner Associates).

3. Results and discussion

3.1. X-ray diffraction

Fig. 1a–c shows the X-ray diffraction patterns for $LiNi_{0.5}Co_{0.44}Fe_{0.06}VO_4$, $LiNi_{0.5}Co_{0.5}VO_4$ heat treated at 723 K for 5 h in air, and the JCPDS 38-1395 data of $LiNiVO_4$, respectively. From Fig. 1a and b, it is evident that the crystalline

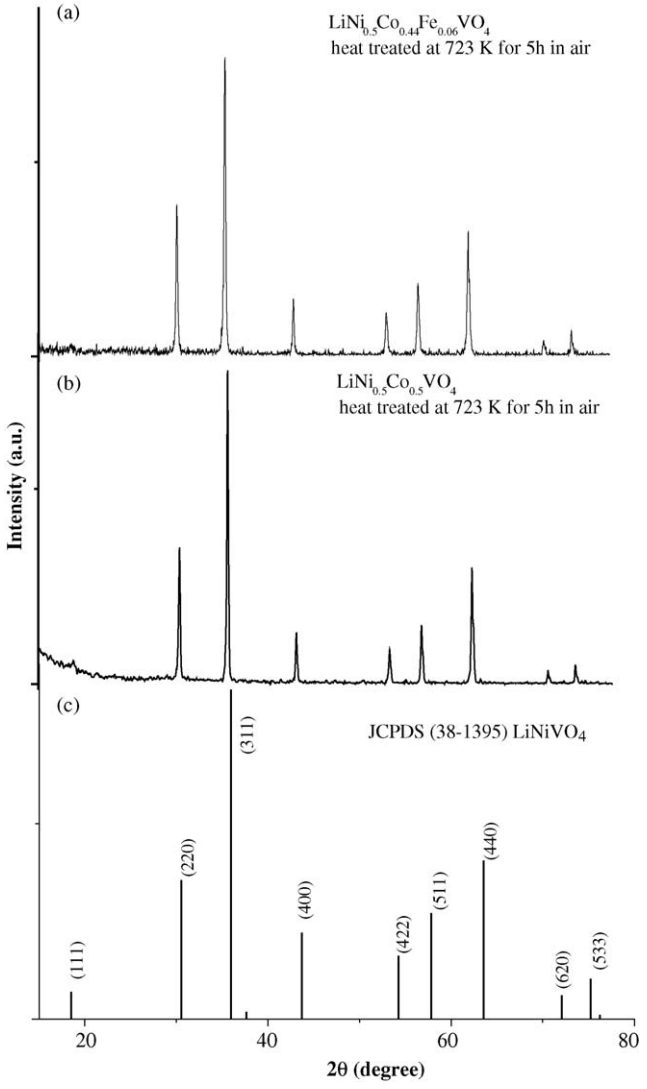

Fig. 1. XRD patterns for (a) $LiNi_{0.5}Co_{0.44}Fe_{0.06}VO_4$, (b) $LiNi_{0.5}Co_{0.5}VO_4$ prepared by CA:PEG (3:1) polymeric route and heat treated at 723 K for 5 h and (c) JCPDS (38-1395) $LiNiVO_4$.

single phase material was obtained after calcinations at 723 K for 5 h in air. The single phase purity of the synthesized $LiNi_{0.5}Co_{0.44}Fe_{0.06}VO_4$ and $LiNi_{0.5}Co_{0.5}VO_4$ compounds was indexed according to the structure with JCPDS file no. 38-1395, a pattern that belongs to an inverse spinel structure with $Fd\bar{3}m(O_h^7)$ space group symmetry. The identifying characteristic of an inverse spinel structure is the ratio of intensities of the (1 1 1) Bragg peaks and a strong (2 2 0) line [1].

The presence of transition metal atoms on the tetrahedral coordinated 8a site leads to an increase in the (2 2 0) intensity at the expense of the (1 1 1) peak. The 0.5 intensity ratio $I(2\,2\,0)/I(3\,1\,1)$ Bragg lines indicates the high crystalline nature of the powders, which were obtained for the samples heat treated at 723 K. The calculated lattice constant a value for the $LiNi_{0.5}Co_{0.5}VO_4$ and $LiNi_{0.5}Co_{0.44}Fe_{0.06}VO_4$ samples were 8.189 and 8.226 Å, respectively, and are consistent with the reported pristine $LiNiVO_4$ and $LiCoVO_4$ samples. The increased lattice constant of the $LiNi_{0.5}Co_{0.44}Fe_{0.06}VO_4$ sample may be due to the substitution Co^{2+} ions by a large ionic radius of Fe^{2+} ions in the tetrahedral sites.

Fig. 2a and b shows the X-ray diffraction patterns for 1.0 wt.% Al_2O_3 coated $LiNi_{0.5}Co_{0.44}Fe_{0.06}VO_4$ synthesized at 873 K for 2 h in air and a pristine sample, respectively. The XRD peak positions were the same and there was no appearance of any new phase peak corresponding to the Al_2O_3. Hence, from the XRD results it can be concluded that the surface coated Al_2O_3 formed a very low concentration and thin layer on the core material, and so did not reveal any corresponding peak.

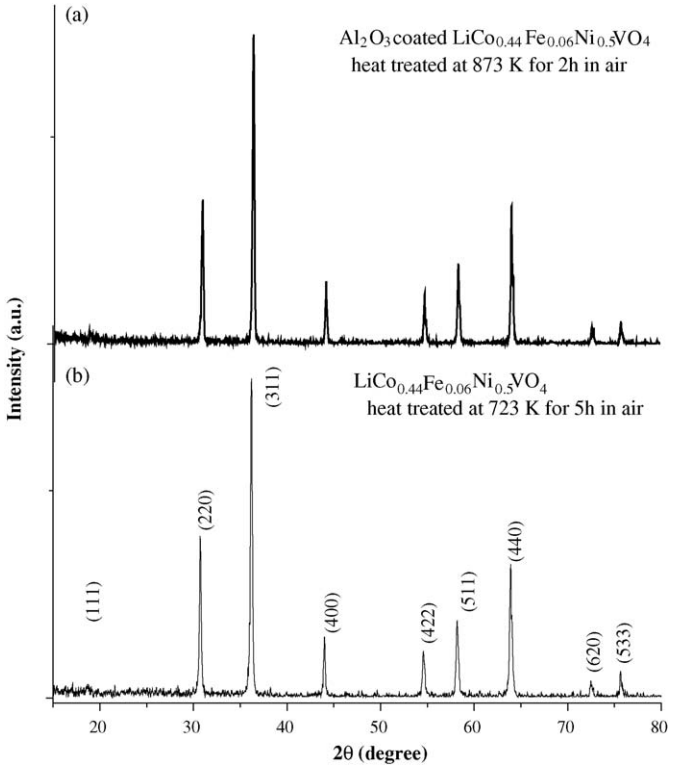

Fig. 2. XRD patterns for (a) 1.0 wt.% Al_2O_3 coated $LiNi_{0.5}Co_{0.44}Fe_{0.06}VO_4$ and (b) $LiNi_{0.5}Co_{0.44}Fe_{0.06}VO_4$ prepared by CA:PEG (3:1) heat treated at 723 K for 5 h.

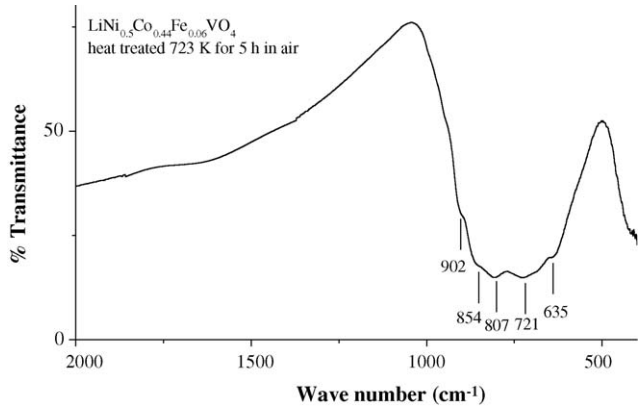

Fig. 3. FTIR spectra for the $LiNi_{0.5}Co_{0.44}Fe_{0.06}VO_4$ heat treated at 723 K.

3.2. FTIR

Fig. 3, shows the FTIR spectrum for the $LiNi_{0.5}Co_{0.44}Fe_{0.06}VO_4$ heat treated at 723 K for 5 h. The citrate and polyethylene complex bands completely disappeared and a pure crystalline $LiNi_{0.5}Co_{0.44}Fe_{0.06}VO_4$ compound was formed. There is a broad strong band in the region 900–550 cm^{-1} that can be assigned to a stretching vibration between the oxygen and V^{5+} ions of the VO_4 tetrahedron, which has A_1 symmetry. The band observed in the region 900–550 cm^{-1} is comprised of sub bands at 894, 852, 794, 727 and 631 cm^{-1}, which were shifted slightly compared with the reported values of $LiNiVO_4$ [8]. This shift in band positions is attributed to substitution of Co and Fe ions in the lattice. The broadness of the 900–550 cm^{-1} band could be tentatively explained in terms of the asymmetrical bonding of the VO_4 tetrahedron, in which four types of cations, namely Li, Co, Ni and Fe, may be bonded with each oxygen atom of a VO_4 tetrahedron. As a result, some symmetry is introduced into the VO_4 unit without disturbing the overall cubic symmetry of the elementary unit cell.

3.3. TGA

Fig. 4 shows the TGA and DTGA data curves for the $LiNi_{0.5}Co_{0.44}Fe_{0.06}VO_4$ polymeric precursor. The TGA curve

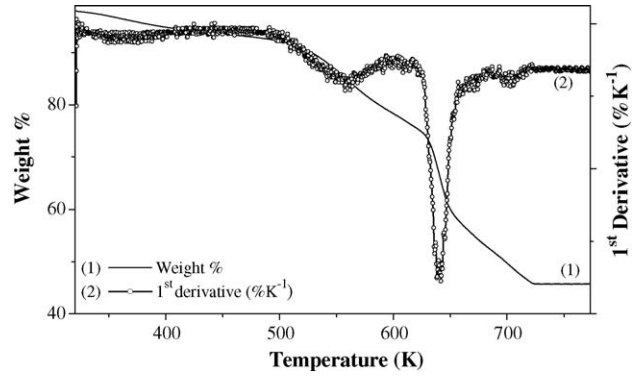

Fig. 4. TGA and DTGA of the $LiNi_{0.5}Co_{0.44}Fe_{0.06}VO_4$ prepared by CA:PEG (3:1) polymeric route.

shows a step-wise weight loss in the temperature ranges from 323–410 K, 480–598 K, 620–670 K and 690–715 K, but there was no weight loss after 723 K. The initial weight loss of 4% is attributed to the loss of water and an excess of free citric acid and other organic residues. In the temperature range 480–598 K, the decomposition of the complex into intermediate and the formation of crystalline $LiNi_{0.5}Co_{0.44}Fe_{0.06}VO_4$ compound, corresponds to the second stage of weight loss of 24%. From 620-670 K and 690–715 K, the full decomposition of the intermediate occurs and the complete phase pure $LiNi_{0.5}Co_{0.44}Fe_{0.06}VO_4$ is formed. The major combustion process was initiated at 620–670 K, as evidenced by the larger DTGA curves. The weight loss stopped at 723 K and these results were supported by XRD results. The 0.5 intensity ratio of $I(2\,2\,0)/I(3\,1\,1)$ Bragg lines indicates the highly crystalline nature of the sample powder calcined at 723 K for 5 h in air. The complete formation of crystalline $LiNi_{0.5}Co_{0.44}Fe_{0.06}VO_4$ at 723 K is also confirmed by FTIR and XRD results, which agree with the results obtained from the TGA/DTGA.

3.4. Morphology

3.4.1. SEM

Fig. 5a and b, characterizes the SEM micrographs for the $LiNi_{0.5}Co_{0.44}Fe_{0.06}VO_4$ cathode material heat treated at 423 K for 24 h and 573 K for 3 h, respectively. From Fig. 5a, it is observed that the morphology of 423 K heat treated sample contains large particles with sharp edges. Fig. 5b, sample heat treated at 573 K revealed these large particles started to break up into flake like structures, due to the decomposition of the complexes as evidenced from Fig. 4 TGA results. In Fig. 5b, the samples were found to be highly porous nature due to the citric acid and PEG polymeric network, in which the metal ions are randomly distributed.

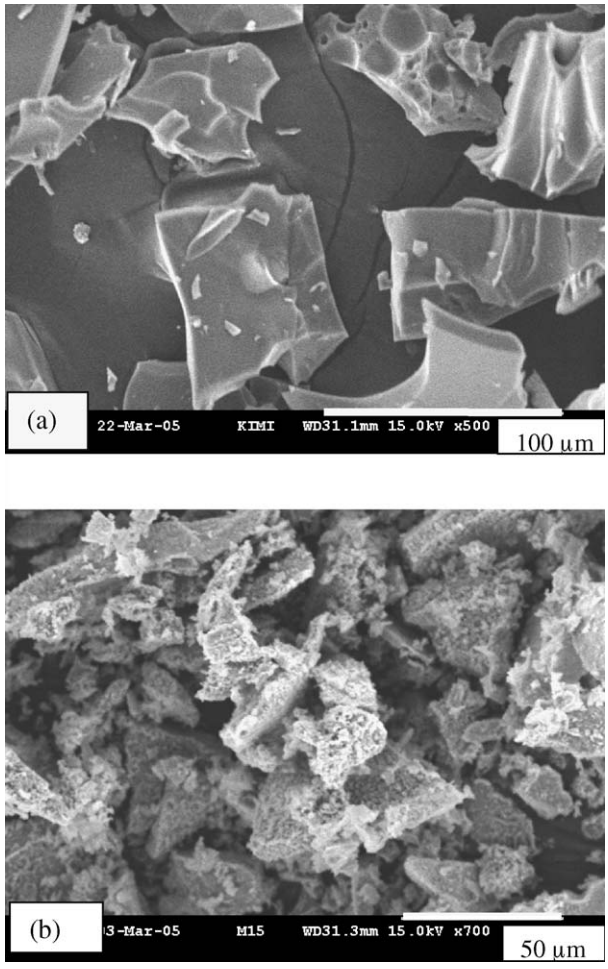

Fig. 5. SEM micrographs of the $LiNi_{0.5}Co_{0.44}Fe_{0.06}VO_4$ powders prepared by CA:PEG (3:1) polymeric route at different temperatures: (a) 423 K (24 h) and (b) 573 (3 h).

3.4.2. TEM

Fig. 6a and b shows the TEM micrographs of $LiNi_{0.5}Co_{0.44}Fe_{0.06}VO_4$ and Al_2O_3 coated $LiNi_{0.5}Co_{0.44}Fe_{0.06}VO_4$ cathode materials, respectively. From Fig. 6a, it is evident that $LiNi_{0.5}Co_{0.44}Fe_{0.06}VO_4$ crystallines are spherical submicron particles with better dispersivity. The average size of these submicron particle ranges from 130 to 150 nm. During the synthesis, particle aggregation was controlled through citric acid and PEG complex network during heat treatment. In Fig. 6b, the Al_2O_3 coating formed translucent compact layer over the core $LiNi_{0.5}Co_{0.44}Fe_{0.06}VO_4$ particles (dark opaque region) and the thickness of the coated layer was around ~15 nm.

3.5. Electrochemical properties

3.5.1. Galvanostatic cycling

Fig. 7 shows the charge–discharge curves of the $LiNi_{0.5}Co_{0.44}Fe_{0.06}VO_4$ cathode material. The initial charge capacities of $LiNi_{0.5}Co_{0.44}Fe_{0.06}VO_4$ materials synthesized with 3:1 CA:PEG content were 87 mAh g^{-1} and they discharged 60 mAh g^{-1}. After 10 cycles, the discharge capacity was 52 mAh g^{-1} with a cycling efficiency of 80% for the first 10 cycles. We preset a cut-off value of 50% capacity retention, calculated with the first-cycle discharge capacity of the respective material, to compare with the number of cycles the cathode materials could sustain. Based on this cut-off regime, the $LiNi_{0.5}Co_{0.44}Fe_{0.06}VO_4$ synthesized with 3:1 CA:PEG contents could sustain up to 31 cycles. Mai et al. [9] reported $LiNi_{0.5}Co_{0.5}VO_4$ cycling efficiency was 43%. Therefore, the Fe doped $LiNi_{0.5}Co_{0.5}VO_4$ in the present study is an improvement over the cycling efficiency of undoped $LiNi_{0.5}Co_{0.5}VO_4$. Therefore, we report that $LiNi_{0.5}Co_{0.44}Fe_{0.06}VO_4$ cathode material with the best capacity retention could be synthesized by a 3:1 CA:PEG polymeric method.

In our present study, the compound synthesized with 3:1 CA:PEG content showed an initial drop in the discharge capacity to 27 mAh g^{-1}. In other words, the irreversible capacity loss was very high, but its capacity retention was good for further cycles compared to reported high voltage $LiNiVO_4$ and $LiNi_{0.5}Co_{0.5}VO_4$, cathode materials [1–5,9]. A possible explanation is the expansion of the lattice in the iron doped sample that is favorable for the Li^+ (de)intercalation process. The composition of the compound, the dopant of Co and Fe ions substituting for Ni ions, and the preparation method are crucial to

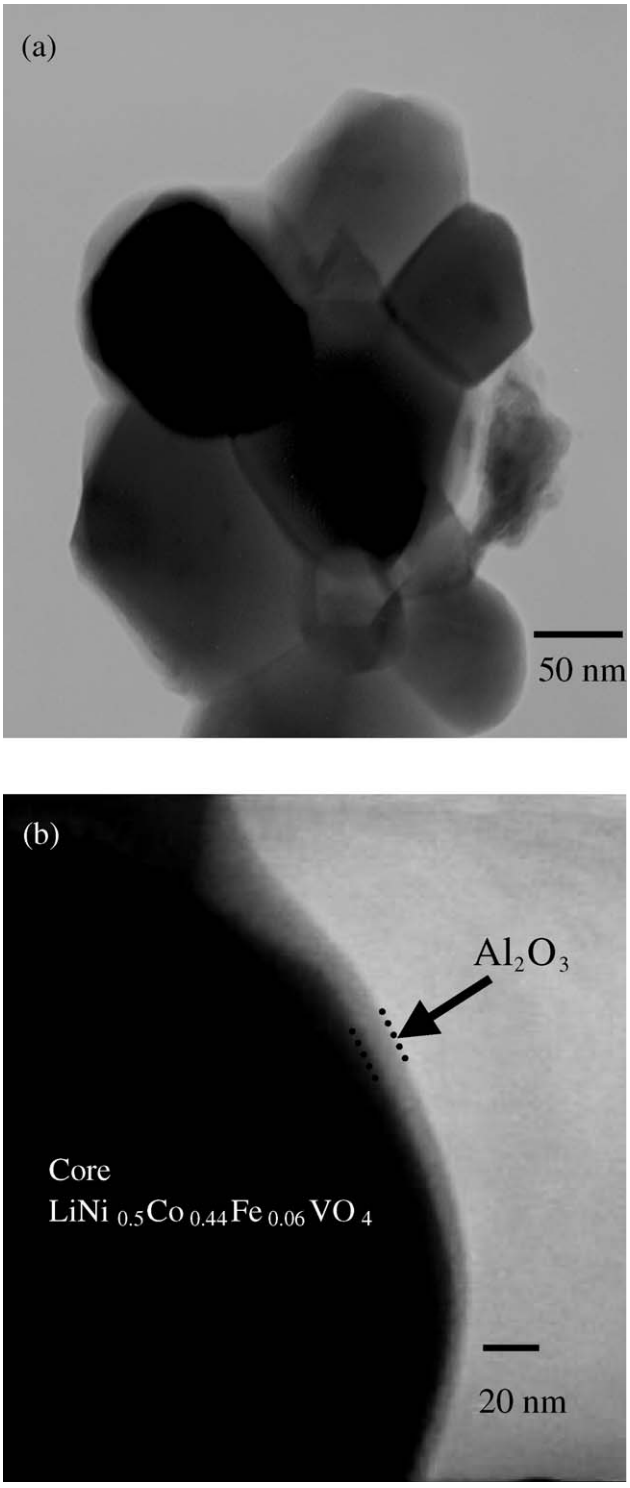

Fig. 6. TEM micrographs of (a) $LiNi_{0.5}Co_{0.44}Fe_{0.06}VO_4$ heated at 723 K for 5 h and (b) 1.0 wt.% Al_2O_3 coated $LiNi_{0.5}Co_{0.44}Fe_{0.06}VO_4$ cathode material heated at 873 K for 2 h.

obtaining a high capacity retention and high voltage cathode material.

Fig. 8 shows the voltage versus capacity plot for 1.0 wt.% Al_2O_3 coated $LiNi_{0.5}Co_{0.44}Fe_{0.06}VO_4$ sample heated at 873 K, during the first 10 cycles at a 0.15 C rate. From Fig. 8, it is observed that there is a plateau around 4.3 V of the

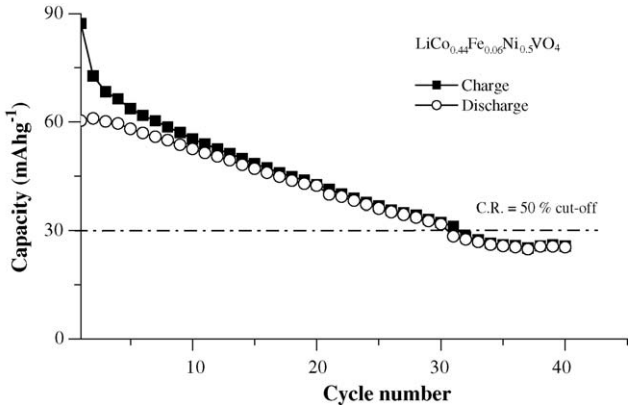

Fig. 7. Cycling behavior of $LiNi_{0.5}Co_{0.44}Fe_{0.06}VO_4$ cathode material. Charge–discharge: 0.15 C rate between 2.8 and 4.9 V.

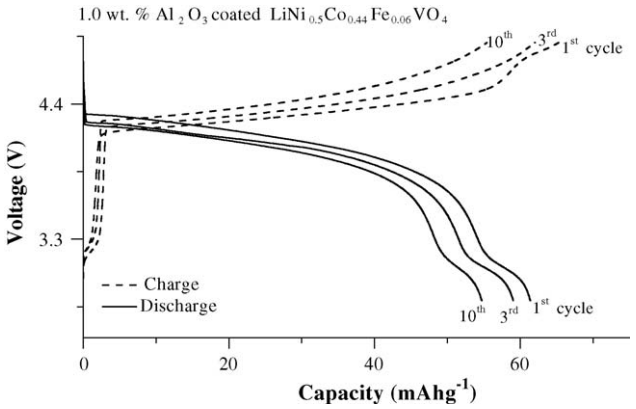

Fig. 8. Charge–discharge curves between 2.8 and 4.9 V for 1.0 wt.% Al_2O_3 coated $LiNi_{0.5}Co_{0.44}Fe_{0.06}VO_4$ sample heated at 873 K, during the first 10 cycles at 0.15 C rate.

charge–discharge profile. Fig. 9, shows the charge–discharge curves of the pristine $LiNi_{0.5}Co_{0.44}Fe_{0.06}VO_4$ and 1.0, 2.5 and 5.0 wt.% Al_2O_3 coated $LiNi_{0.5}Co_{0.44}Fe_{0.06}VO_4$. Table 1, presents the initial charge and discharge capacities of the pristine, 1.0, 2.5 and 5.0 wt.% Al_2O_3 coated $LiNi_{0.5}Co_{0.44}Fe_{0.06}VO_4$ materials and also their cycle efficiency. Table 1 illustrates that there may be a large irreversible capacity loss of the pristine material compared to the coated

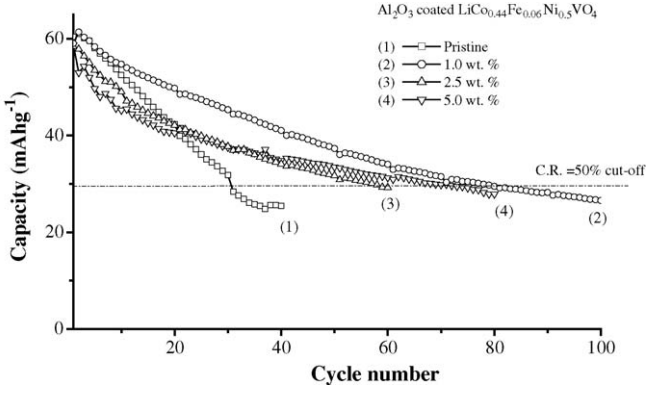

Fig. 9. Cycling behavior of various wt.% Al_2O_3 coated $LiNi_{0.5}Co_{0.44}Fe_{0.06}VO_4$ cathode material. Charge–discharge: 0.15 C rate between 2.8 and 4.9 V.

Table 1
A comparison of capacity data of the pristine and various wt.% Al_2O_3 coated $LiNi_{0.5}Co_{0.44}Fe_{0.06}VO_4$ cycled between 2.8–4.9 V at 0.15 C rate

Cathode materials	Initial charge capacity ($mAh\,g^{-1}$)	Initial discharge capacity ($mAh\,g^{-1}$)	Initial cycle efficiency (%)
Pristine $LiNi_{0.5}Co_{0.44}Fe_{0.06}VO_4$	87	60	70
1.0 wt.% Al_2O_3 coated $LiNi_{0.5}Co_{0.44}Fe_{0.06}VO_4$	65	60	92
2.5 wt.% Al_2O_3 coated $LiNi_{0.5}Co_{0.44}Fe_{0.06}VO_4$	64	58	90
5.0 wt.% Al_2O_3 coated $LiNi_{0.5}Co_{0.44}Fe_{0.06}VO_4$	67	59	88

samples. The coated samples also exhibited a lower initial capacity at various coating levels, due to the presence of inactive Al_2O_3 on the electrode.

From Fig. 9, it is observed that the coating improved the cycle stability of the cathode material. According to a preset cut-off value of 50 % for the capacity retention, pristine $LiNi_{0.5}Co_{0.44}Fe_{0.06}VO_4$ could sustain just 31 cycles, but the samples coated with 1.0, 2.5 and 5.0 wt.% sustained 80, 57 and 68 cycles, respectively. However, when the coating level was increased further to 2.5 and 5.0 wt.%, the cycle stability decreased. At the higher coating level, the cathode particles were partially insulated, thereby lowering the capacity utilization and cycle stability. The presence of excess coating material between the particles could also lower the particle-to-particle electronic conductivity, adversely affecting the coulombic efficiency. According to Courtright [22], thinner coatings produce smaller cracks that are a factor in controlling the ingress of molecular species. The 1.0 wt.% Al_2O_3 coated sample was found to possess cycle stability 2.6 times better than the pristine cathode material.

The enhanced cycle stability is attributed the Al_2O_3 coating that shields the surface of the core material against HF attack at high voltages up to 4.9 V. Thackeray et al. [23] reported that the improved cycle stability of ZrO_2 coated $LiMn_2O_4$ is because ZrO_2 acts as an amphoteric surface that scavenges the acidic HF species from the $LiPF_6$ liquid electrolyte. In the present study, this explanation holds relatively well since Al_2O_3 is also amphoteric oxide. Therefore, it is not surprising that coated samples have better cycle stability compared to pristine samples.

3.5.2. Electrochemical impedance

Electrochemical impedance spectroscopy (EIS) is a powerful method for studying electrochemical mechanisms, especially in the field of lithium ion batteries [24]. The EIS response for the pristine and 1.0 wt.% Al_2O_3 coated $LiNi_{0.5}Co_{0.44}Fe_{0.06}VO_4$ cathodes in non-aqueous electrolytes was conducted to understand the electrochemical performance of the compounds with the electrode kinetics. The spectra reveal the processes, such as the transport of lithium ions in the electrolyte, charge-transfer across the electrode/electrolyte interface, and adsorption of absorbed lithium ions into the solid oxide matrix [25,26]. Fig. 10a and b shows the EIS profiles of the pristine and 1.0 wt.% of Al_2O_3 coated $LiNi_{0.5}Co_{0.44}Fe_{0.06}VO_4$ cathode materials charged at 4.9 V as function of various cycles. In Fig. 10a and b, the high frequency semicircle represents the impedance due to the solid-state interface layer formed on the surface of the electrodes and the low-frequency semicircle is related to a faradic slow charge transfer resistance at the interface and its relative double-layer capacitance. The straight sloping line at the low frequency end is a Warburg tail that implies a combination of the diffusional effects of lithium ion on the interface between the active material particles and electrolyte.

From Fig. 10a and b, it is observed that the solution resistance, R_e, undergoes very small changes upon cycling from 2.7 to 7.1 Ω and 3.7 to 6.1 Ω for the pristine and coated samples. The slight changes in solution resistance are attributed to the complex chemistry of lithium in electrolyte solutions that leads to slight changes in the content of the conducting species in the solution [27]. However, the size of the semicircle increased upon cycling and in the case of the uncoated samples, they increase even more, as shown in Fig. 10a. From Fig. 10a and b, the resistances of the high frequency semicircle of the cathode materials as a function of cycle number showed that the resistances of the surface film on the cathode particles were 24, 83, 163 and 178 Ω for the 1st,

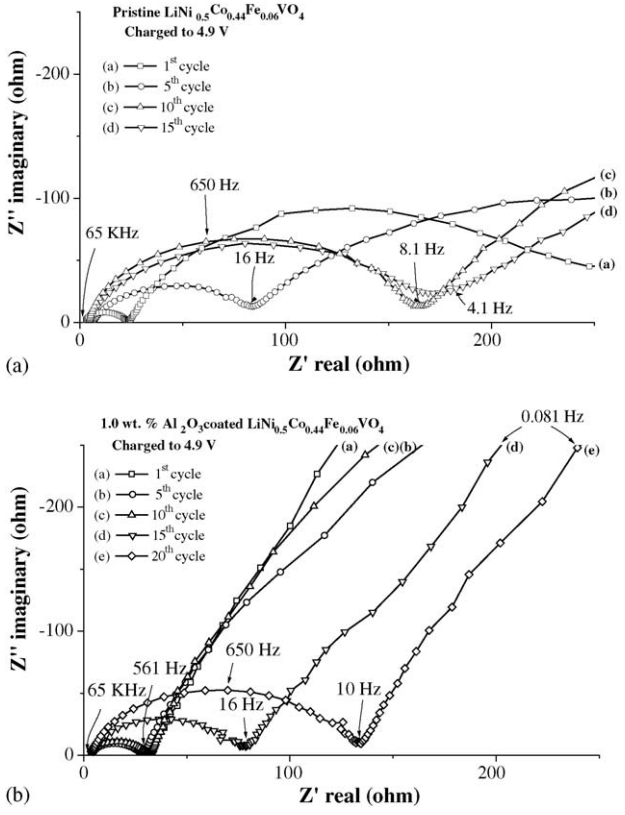

Fig. 10. Electrochemical impedance plots of (a) $LiNi_{0.5}Co_{0.44}Fe_{0.06}VO_4$ and (b) 1.0 wt.% Al_2O_3 coated $LiNi_{0.5}Co_{0.44}Fe_{0.06}VO_4$ sample as a function of cycle number.

5th, 10th and 15th cycles, respectively, for the uncoated sample. The 1.0 wt.% Al_2O_3 coated $LiNi_{0.5}Co_{0.44}Fe_{0.06}VO_4$ showed an increase in resistance to 31, 27, 32, 78 and 133 Ω for the 1st, 5th, 10th, 15th and 20th cycles, respectively. The impedance results revealed that a compact surface film of polycarbonates, alkyl carbonates and LiF [28–30] was formed. The composition of this film changes as the reaction products of the oxide are incorporated with the electrolyte constituents. Thus, during repeated cycling, a fast inactive surface film gets transformed into a thick dense layer, resulting in impedance growth that renders it inactive for the electrochemical reaction in the pristine material. XPS analysis [31] concluded that the cathode material surface is formed of organic species and their reactions with the lithium-salt anion are more dependent on electrode material type. It is especially important to reduce the impact of the PF_6 anion and its related contaminants (HF and PF_5) on electrode surface chemistry through the implementation of more stable salts. According to Aurbach et al. [32], although $LiCoO_2$ cathodes undergo a gradual degradation upon cycling, the major capacity fade mechanism involves the formation and thickening of surface films.

4. Conclusions

$LiNi_{0.5}Co_{0.44}Fe_{0.06}VO_4$ cathode material was successfully synthesized by a CA:PEG polymeric method and surface coated with Al_2O_3. XRD results revealed that complete crystallization occurred at a low temperature of 723 K. FTIR spectrum results demonstrated that the organic residues were completely removed at low temperatures, which was also evident in TGA data. SEM micrographs showed the morphology of the materials at different stages of compound synthesis. TEM micrographs showed uniform sub-micron sized particles and the thickness of the coated layer on the core material. The electrochemical measurements of $Li/LiNi_{0.5}Co_{0.44}Fe_{0.06}VO_4$ cells demonstrated good cell performance at a high voltage of 4.9 V. The cell performance of $LiNi_{0.5}Co_{0.44}Fe_{0.06}VO_4$ synthesized with CA:PEG content sustained 31 cycles and the1.0 wt.% Al_2O_3 coated $LiNi_{0.5}Co_{0.44}Fe_{0.06}VO_4$ sustained 80 cycles. Electrical impedance spectra of the cathode suggest that interaction with the electrolyte during electrochemical cycling results in shorter cycle life due to the resistance offered by impedance growth on the pristine material.

Acknowledgements

Financial support for this work was provided by the National Science Council of the Republic of China under contract No. NSC 93-2214-E-008-004. PMD thanks the NSC for the award of a post-doctoral fellowship.

References

[1] G.T.K. Fey, W. Li, J.R. Dahn, J. Electrochem. Soc. 141 (1994) 227.
[2] G.T.K. Fey, W.B. Perng, Mater. Chem. Phys. 47 (1997) 279.
[3] G.T.K. Fey, C.S. Wu, J. Pure Appl. Chem. 69 (1997) 329.
[4] G.T.K. Fey, Kuo-Song Chen, J. Power Sources 81/82 (1999) 467.
[5] G.T.K. Fey, D.-L. Huang, Electrochim. Acta 45 (1999) 295.
[6] C.-H. Lu, W.-C. Lee, S.-J. Liou, G.T.K. Fey, J. Power Sources 81/82 (1999) 696.
[7] G.T.K. Fey, K.S. Wang, S.M. Yang, J. Power Sources 68 (1997) 159.
[8] C. Julien, M. Massot, C. Peřrez-Vicente, Mater. Sci. Eng. B75 (2000) 6.
[9] L.-Q. Mai, W. Chen, Q. Xu, Q.-Y. Zhu, C.-H. Han, W.-L. Guo, Solid State Ionics 161 (2003) 205.
[10] N. Van Landschoot, E.M. Kelder, P.J. Kooyman, C. Kwakernaak, J. Schoonman, J. Power Sources 138 (1/2) (2004) 262.
[11] N. Van Landschoot, E.M. Kelder, J. Schoonman, Solid State Ionics 166 (3/4) (2004) 307.
[12] N. Van Landschoot, C. Kwakernaak, W.G. Sloof, E.M. Kelder, J. Schoonman, J. Eur. Ceram. Soc. 25 (2005) 3469.
[13] J. Cho, Y.J. Kim, B. Park, Chem. Mater. 12 (2000) 3788.
[14] J. Cho, Y.J. Kim, B. Park, J. Electrochem. Soc. 148 (2001) A1110.
[15] J. Cho, Y.J. Kim, T.-J. Kim, B. Park, Angew. Chem. Int. Ed. 40 (2001) 3367.
[16] L. Liu, Z. Wang, H. Li, L. Chen, X. Huang, Solid State Ionics 152/153 (2002) 341.
[17] A.M. Kannan, L. Rabenberg, A. Manthiram, Electrochem. Solid-State Lett. 6 (2003) A16.
[18] G.T.K. Fey, Z.X. Weng, J.G. Chen, C.Z. Lu, T. Prem Kumar, S.P. Naik, A.S.T. Chiang, D.C. Lee, J.R. Lin, J. Appl. Electrochem. 34 (2004) 715.
[19] Z. Wang, C. Wu, L. Liu, F. Wu, F. Wu, L. Chen, X. Huang, J. Electrochem. Soc. 149 (2002) A466.
[20] J. Cho, Y.J. Kim, T.-J. Kim, B. Park, Angew. Chem. Int. Ed. 40 (2001) 3367.
[21] G.T.K. Fey, H.Z. Yang, T.P. Kumar, S.P. Naik, A.S.T. Chiang, D.C. Lee, J.R. Lin, J. Power Sources 132 (1/2) (2004) 172.
[22] E.L. Courtright, Surf. Coat. Technol. 68/69 (1994) 116.
[23] M.M. Thackeray, C.S. Johnson, J.-S. Kim, K.C. Lauzze, J.T. Vaughey, N. Dietz, D. Abraham, S.A. Hackney, W. Zeltner, M.A. Anderson, Electrochem. Commun. 5 (2003) 752.
[24] D.A. Harrington, P. van den Driessche, J. Electroanal. Chem. 567 (2004) 153.
[25] F. Croce, F. Nobili, A. Deptula, W. Lada, R. Tossici, A. D'Epifanio, B. Scrosati, R. Marassi, Electrochem. Commun. 1 (1999) 605.
[26] F. Nobili, F. Croce, B. Scrosati, R. Marassi, Chem. Mater. 13 (2001) 1642.
[27] D. Aurbach, A. Schechter, Electrochim. Acta 46 (2001) 2395.
[28] D. Aurbach, M.D. Levi, E. Levi, H. Teller, B. Markovsky, G. Salitra, L. Heider, U. Heider, J. Electrochem. Soc. 145 (1998) 3024.
[29] D. Aurbach, B. Markovsky, M.D. Levi, E. Levi, A. Schechter, M. Moshkovich, Y.S. Cohen, J. Power Sources 81/82 (1999) 95.
[30] D. Aurbach, B. Markovsky, A. Rodkin, E. Levi, Y.S. Cohen, H.J. Kim, M. Schmidt, Electrochim. Acta 47 (2002) 4291.
[31] K. Edstrom, T. Gustafsson, J.O. Thomas, Electrochim. Acta 50 (2/3) (2004) 395.
[32] D. Aurbach, B. Markovsky, A. Rodkin, M. Cojocaru, E. Levi, H.J. Kim, Electrochim. Acta 47 (2002) 1899.